



*Geoscientific Model Development Discussions* is the access reviewed discussion forum of *Geoscientific Model Development*

# Quantifying atmospheric transport, chemistry, and mixing using a new trajectory-box model and a global atmospheric-chemistry GCM

H. Riede, P. Jöckel, and R. Sander

Max Planck Institute for Chemistry, Air Chemistry Department, P.O. Box 3060,  
55020 Mainz, Germany

Received: 22 April 2009 – Accepted: 24 April 2009 – Published: 8 May 2009

Correspondence to: H. Riede (hella.riede@mpic.de)

Published by Copernicus Publications on behalf of the European Geosciences Union.

## Quantifying atmospheric transport, chemistry, and mixing

H. Riede et al.

Title Page

Abstract

Introduction

Conclusions

References

Tables

Figures



Back

Close

Full Screen / Esc

Printer-friendly Version

Interactive Discussion

## Abstract

We present a novel method for the quantification of transport, chemistry, and mixing along atmospheric trajectories based on a consistent model hierarchy. The hierarchy consists of the new atmospheric-chemistry trajectory-box model CAABA/MJT and the three-dimensional (3-D) global ECHAM/MESSy atmospheric-chemistry (EMAC) general circulation model (GCM). CAABA/MJT employs the atmospheric box model CAABA together with the atmospheric-chemistry submodel MECCA (M), the photochemistry submodel JVAL (J), and the new trajectory submodel TRAJECT (T), to simulate atmospheric chemistry along atmospheric trajectories which are provided off-line. With the same submodels coupled to the EMAC model, a unique consistency is achieved, which allows to separate contributions of transport, chemistry, and mixing along the trajectory pathways through comparison of results from the two models. Consistency of transport between the trajectory-box model CAABA/MJT and the 3-D EMAC model is achieved via calculation of trajectories based on 3-D wind fields from EMAC. The procedure to obtain the necessary statistical basis for the quantification analysis is described as well as the comprehensive diagnostics with respect to chemistry. The quantification method is applied to 3-D model data as a diagnostic tool with the focus on the transfer of results to observational data.

## 1 Introduction

Transport, mixing, and chemistry are complex key processes which determine the distribution of chemical species within the atmosphere. Given the concentrations of chemical species observed at a certain point in time and space, the quantification of contributions of the respective processes is often only partially possible. Analyses of the correlations and lifetimes of shorter-lived species can help to assess the relative effects of mixing and chemistry in some cases, but given the complexity of the atmospheric environment, we present a new method to quantify the contributions of transport, mix-

**GMDD**

2, 455–484, 2009

## Quantifying atmospheric transport, chemistry, and mixing

H. Riede et al.

[Title Page](#)

[Abstract](#)

[Introduction](#)

[Conclusions](#)

[References](#)

[Tables](#)

[Figures](#)

[⏪](#)

[⏩](#)

[◀](#)

[▶](#)

[Back](#)

[Close](#)

[Full Screen / Esc](#)

[Printer-friendly Version](#)

[Interactive Discussion](#)

ing and chemistry with a consistent model hierarchy. We consequently further developed the idea of separation of the different contributions within a grid-based model (e.g., Arteta and Cautenet, 2007) to a Lagrangian method by the introduction of the trajectory-box model CAABA/MJT with maximum consistency to the 3-D grid-based EMAC model. Quantification results allow to investigate the transport and mixing characteristics of a grid-based 3-D model and complement observations with additional information about the history of observed air masses.

Several zero- and one-dimensional model types are currently employed in atmospheric research, among them atmospheric-chemistry box models to investigate chemical and photochemical processes at a certain location, e.g., MECCA (Sander et al., 2005), trajectory models to investigate atmospheric transport pathways of air parcels, e.g., LAGRANTO (Wernli and Davies, 1997), TRAJKS (Scheele et al., 1996), and FLEXTRA (Stohl et al., 1995), Lagrangian particle dispersion models, e.g., FLEXPART (Stohl et al., 2005), and combinations thereof, e.g., CLaMS (McKenna et al., 2002), and BRAPHO (Sinnhuber et al., 1999). All of these models have been designed for their own special purpose. The specialty of the trajectory-box model CAABA/MJT presented here is its comprehensive and flexible chemical mechanism provided by MECCA and its unique consistency with the global three-dimensional (3-D) ECHAM/MESSy atmospheric chemistry (EMAC) model (Jöckel et al., 2006).

## 2 Methodology – the model hierarchy

We employ a model hierarchy consisting of the 3-D EMAC model and the atmospheric-chemistry box model CAABA (Sander et al., 2009). Both models were developed within the MESSy framework (Jöckel et al., 2005), which allows flexible coupling of the same submodels to various base models, as shown here for CAABA and EMAC, so that an exceptionally high consistency between the model setups is achieved (see Fig. 1).

The trajectory-box model setup presented in this publication employs CAABA as base model and uses three submodels: the submodel MECCA to simulate atmo-

## Quantifying atmospheric transport, chemistry, and mixing

H. Riede et al.

[Title Page](#)

[Abstract](#)

[Introduction](#)

[Conclusions](#)

[References](#)

[Tables](#)

[Figures](#)



[Back](#)

[Close](#)

[Full Screen / Esc](#)

[Printer-friendly Version](#)

[Interactive Discussion](#)



spheric chemistry, the submodel JVAL to determine photolysis rate coefficients, and the new submodel TRAJECT for the processing of trajectory information. This is the combination of submodels presently referenced as CAABA/MJT. The 3-D EMAC model data were produced using the same submodels MECCA and JVAL. The trajectory-box model is thus suitable for the quantification of contributions and for an on-top analysis of chemical events within the 3-D model, which are described in the next paragraphs and in Sect. 4.1, respectively.

We use combinations and comparisons of results from CAABA/MJT and from EMAC to determine the contributions of mixing, chemistry and transport along trajectories, which are provided offline. Figure 2 shows the applied models and their spatial regimes.

The quantification is individual for each tracer  $M$ . The mixing ratio  $\mu_M$  initialised at the beginning of a trajectory, interpolated from EMAC grid-based results at the corresponding position in time ( $t=t_0$ ) and space ( $\mathbf{r}=\mathbf{r}_0=(x_0, y_0, z_0)$ ), defines the theoretical influence of undisturbed transport ( $\mu_{M,\text{trans}}$ ). Subsequently, the system of chemical kinetic equations is solved within CAABA/MJT forward in time along the trajectory. The differences of mixing ratios between start ( $t_0$ ) and end ( $t=t_E$ ) of the trajectory define the contributions of chemistry ( $\Delta\mu_{M,\text{chem}}$ ). Finally, due to the high consistency between the box model CAABA/MJT and the 3-D EMAC model, it is possible to attribute differences in tracer mixing ratios between the two models at the end of a trajectory to mixing, the only fundamental difference ( $\Delta\mu_{M,\text{mix}}$ ).

In conclusion, the mixing ratio of a species at the beginning of a trajectory represents the theoretical contribution of transport as known from passive tracers. It is subsequently modified by pure chemistry through CAABA/MJT and by mixing as implemented in EMAC. Figure 3 and the following equations, in which CAABA/MJT is abbreviated as CAABA, summarise the above description:

$$\mu_{M,\text{trans}} = \mu_M(\text{EMAC}(t_0, \mathbf{r}_0)) = \mu_M(\text{CAABA}(t_0)) \quad (1)$$

$$\Delta\mu_{M,\text{chem}} = \mu_M(\text{CAABA}(t_E)) - \mu_M(\text{CAABA}(t_0)) \quad (2)$$

## Quantifying atmospheric transport, chemistry, and mixing

H. Riede et al.

Title Page

Abstract

Introduction

Conclusions

References

Tables

Figures

⏪

⏩

◀

▶

Back

Close

Full Screen / Esc

Printer-friendly Version

Interactive Discussion

$$\Delta\mu_{M,\text{mix}} = \mu_M(\text{EMAC}(t_E, r_E)) - \mu_M(\text{CAABA}(t_E)) . \quad (3)$$

Trajectories are based on the 3-D wind fields from EMAC to ensure consistency in transport between trajectory-box model and global model. The corresponding boundary conditions used in the trajectory-box model are sampled from the 3-D model along the calculated trajectories. If backward (forward) trajectories are analysed, sensitivity tests can be conducted by variation of the backward (forward) time of the trajectories and corresponding variation of the initialisation (end point). In general, the shorter the trajectory the more congruency to the 3-D model is expected and the fewer trajectories are necessary to represent different transport pathways (see also Sect. 3).

The uncertainty concerning chemistry can be estimated using an ensemble plot showing the mixing ratios of a certain species on several trajectories as shown for the application example (Sect. 5). A detailed analysis of chemical processes is outlined in the model description of CAABA in Sect. 4.1 and exemplarily shown in the application section. Tracers which are chemically inert at the time scales of a few days provide an additional analysis of mixing influences.  $\text{SF}_6$ , for example, is suited to assess anthropogenic influence; its source features no significant seasonal cycle and is purely anthropogenic with a corresponding mixing ratio gradient from North to South and from the source regions up to the free troposphere and beyond.

### 3 Statistical basis and transferability from the model hierarchy analysis to observations

How can the quantification result help to analyse field measurements? As a basis for the transfer of results, a comparison between observational data and data from the 3-D model is mandatory. Only if the general features in the measurement series and in the corresponding data sampled from the 3-D model are in agreement, subsequent analysis using the model hierarchy is meaningful for the interpretation of the selected campaign data.

[Title Page](#)

[Abstract](#)

[Introduction](#)

[Conclusions](#)

[References](#)

[Tables](#)

[Figures](#)

[⏪](#)

[⏩](#)

[◀](#)

[▶](#)

[Back](#)

[Close](#)

[Full Screen / Esc](#)

[Printer-friendly Version](#)

[Interactive Discussion](#)

---

## Quantifying atmospheric transport, chemistry, and mixing

H. Riede et al.

---

Title Page

Abstract

Introduction

Conclusions

References

Tables

Figures



Back

Close

Full Screen / Esc

Printer-friendly Version

Interactive Discussion



As a next step, in addition to the trajectories based on wind fields from the 3-D model, sets of trajectories based on wind fields from a forecast or reanalysis model (e.g., ECMWF<sup>1</sup>, NCEP<sup>2</sup>) are calculated. To ensure a statistical basis for results from the trajectory-box model on the one hand, and an assessment of the portability of results from the model hierarchy to the best available real atmospheric situation on the other hand, the two sets of trajectories are grouped into coherent trajectory bundles. A simple grouping method applied here uses the absolute horizontal transport deviation and the ratio of pressures of the starting points of the back trajectories as thresholds between separate bundles (see also Sect. 5). Of these bundles, a trajectory in the middle is kept as a representative to be used in the trajectory-box model simulation and for further analysis, while the number of all trajectories within the bundle provides its statistical weight. Representative trajectories of the 3-D model as well as the forecast or reanalysis model are then compared. Common methods of comparison between trajectories include the absolute horizontal and vertical transport deviation between single trajectory points and mean errors between whole trajectories, as applied for instance in Stohl et al. (2001) and Knudsen et al. (2001). For a general discussion of trajectory uncertainties, see for example Stohl (1998).

## 4 Model description

### 4.1 CAABA box model and submodels

CAABA, Chemistry As A Box model Application (Sander et al., 2009), is an atmospheric chemistry box model developed within the MESSy framework (Jöckel et al., 2005). In this publication, it is used as base model, to which submodels are coupled via the standardised MESSy interface, for example the submodels MECCA for atmo-

---

<sup>1</sup><http://www.ecmwf.int/>

<sup>2</sup><http://www.ncep.noaa.gov/>

spheric chemistry, or JVAL for photolysis rate coefficients. For the present study, the submodels simulating sedimentation and deposition are switched off.

MECCA, the Module Efficiently Calculating the Chemistry of the Atmosphere (Sander et al., 2005), simulates tropospheric and stratospheric chemistry and photochemistry. The KPP (Kinetic Pre-Processor) software (Sandu and Sander, 2006) is used for the integration of the set of stiff differential equations describing chemistry. Besides the pre-selected chemical mechanisms provided, it is possible to customise the mechanism by simple boolean commands. The mixing ratios of nitrogen ( $N_2$ ), oxygen ( $O_2$ ), and carbon dioxide ( $CO_2$ ), species are fixed during the simulation. In consistency with the application of MECCA in combination with EMAC during the S1 simulation (see Sect. 4.2), aerosol chemistry as described in Kerkweg et al. (2007) was switched off. To facilitate the application case study (Sect. 5), heterogeneous reactions were neglected in the present box model setup. Having achieved a net quantification of transport, mixing, and chemistry, the chemistry submodel MECCA provides information for a more detailed analysis of chemical processes. The inclusion of customised diagnostic tracers (e.g., “loss of ozone”) into the chemical mechanism allows to monitor the overturn of certain species or reaction systems. With all the chemical equations and reaction rates available, a detailed listing of positive and negative contributions of individual reactions to a certain species is possible. This can be calculated for a time period, e.g., the whole trajectory time, or single integration time steps. An example of the first is shown in the application (Sect. 5).

The JVAL submodel is employed for fast online calculation of photolysis rate coefficients accounting for climatological aerosol as well as cloud water content, cloud cover, and ozone either calculated by the base model or provided by a climatology (Landgraf and Crutzen, 1998). A delta-two-stream method is used for eight spectral intervals in the UV and visible together with pre-calculated effective cross-sections, partly temperature and pressure dependent, for more than 50 tropospheric and stratospheric species. Only the photolysis rates for species present in the chosen chemical mechanism are calculated. For the trajectory-box model calculations, the cloud fraction and

## Quantifying atmospheric transport, chemistry, and mixing

H. Riede et al.

[Title Page](#)

[Abstract](#)

[Introduction](#)

[Conclusions](#)

[References](#)

[Tables](#)

[Figures](#)

[⏪](#)

[⏩](#)

[◀](#)

[▶](#)

[Back](#)

[Close](#)

[Full Screen / Esc](#)

[Printer-friendly Version](#)

[Interactive Discussion](#)

cloud water content is set to zero.

We developed CAABA further to include the new trajectory submodel *TRAJECT*, which provides the infrastructure to change physical boundary conditions such as longitude, latitude, pressure, temperature, relative humidity, and photolysis rate coefficients during the calculation of chemical kinetics. As default, the chemistry in CAABA/MJT should perfectly match the chemistry in EMAC, which is easy to achieve for the chemical mechanism. Other influences from the three-dimensional environment onto photochemistry can be accounted for in CAABA/MJT simulations via extended boundary conditions. The external photolysis rates mentioned above, for example, replace information about cloud cover and aerosol optical density.

An external trajectory file in netCDF<sup>3</sup> format provides the boundary conditions for a trajectory on individual waypoints, without requirement for equidistance in time or space. If trajectory waypoints do not coincide with the fixed CAABA integration time steps, additional time steps are inserted around the trajectory point so that the regular time stepping as well as the trajectory waypoints are present in the trajectory-box model output (Fig. 4). Between trajectory waypoints, linear interpolation is applied to the prescribed boundary conditions.

By default, the model simulation time is defined by the length of the trajectory. However, it is possible via two namelist parameters to modify the simulation time period and the start of the simulation along the trajectory so that any section along the trajectory can be chosen, independent of waypoints or time step interval. The minimum number of trajectory points to be provided is two. Figure 5 depicts the applied operator splitting for a trajectory with three trajectory waypoints, of which only an inner section of the trajectory is calculated.

<sup>3</sup><http://www.unidata.ucar.edu/software/netcdf/>

## Quantifying atmospheric transport, chemistry, and mixing

H. Riede et al.

Title Page

Abstract

Introduction

Conclusions

References

Tables

Figures

⏪

⏩

◀

▶

Back

Close

Full Screen / Esc

Printer-friendly Version

Interactive Discussion



## 4.2 EMAC S1 simulation

The ECHAM/MESy Atmospheric Chemistry (EMAC) model is a numerical chemistry and climate software that includes submodels describing tropospheric and middle atmosphere processes and their interactions with oceans, land and human influences (Jöckel et al., 2006). It uses the first version of the Modular Earth Submodel System (MESy1) to link multi-institutional computer codes. The core atmospheric model is the 5th generation European Centre Hamburg general circulation model (ECHAM5, Roeckner et al., 2006). The results from the evaluation reference simulation S1 (Jöckel et al., 2006) used in the present publication were obtained with the ECHAM5 version 5.3.01 and MESy version 1.0 in the T42L90MA resolution, i.e. with a spherical truncation of T42 (corresponding to a quadratic Gaussian grid of approximately 2.8 by 2.8 degrees in latitude and longitude) and with 90 vertical hybrid pressure levels up to 0.01 hPa. The applied model setup comprised the submodels as described in Jöckel et al. (2006), among them MECCA and JVAL. Online emissions include DMS from the oceans, NO from soils and isoprene from plants. Offline emissions are based on the EDGAR<sup>4</sup> emissions database with incorporated fire emissions based on the Global Fire Emissions Database (GFED) for the year 2000. A Newtonian relaxation technique was applied in the free tropospheric part to weakly nudge the model towards the analysed ECMWF meteorology. Thus, direct comparisons between model results and observations become feasible.

## 5 Application example

### 5.1 Dynamic situation

As an example, the quantification method is applied to a five-day back trajectory with hourly waypoints calculated with the 3-D trajectory model LAGRANTO (Wernli and

<sup>4</sup><http://www.mnp.nl/edgar/model/v32ft2000edgar/>

## GMDD

2, 455–484, 2009

### Quantifying atmospheric transport, chemistry, and mixing

H. Riede et al.

Title Page

Abstract

Introduction

Conclusions

References

Tables

Figures

⏪

⏩

◀

▶

Back

Close

Full Screen / Esc

Printer-friendly Version

Interactive Discussion



Davies, 1997) driven by EMAC wind fields. The trajectory was chosen from among the 21 trajectories depicted in Fig. 6, each representative for a coherent bundle as described in Sect. 3. The trajectories show a highly dynamic situation of downdraft and updraft above Africa in January 2000, with a common submergence zone at 10–15°

North following an anticyclonic movement. The subsequent fast westerly movement is a typical climatological feature (see ECMWF ERA-40 Atlas<sup>5</sup>). A comparison with respective trajectories based on ECMWF wind fields (inset of Fig. 6) shows the same anticyclonic movement with a different shape and partly different and lower source regions. The transport pathways crossing the tropical Atlantic are also observed for EMAC trajectories at a later time, approximately shifted by 15 to 30 min (not shown).

The trajectory selected for the sample simulation travels from approximately 290 hPa (~10 km altitude) in the upper troposphere down to below 400 hPa (~7 km) in the free troposphere above the sub-Sahel zone and back up to an airborne observation platform above the Persian Gulf at about 290 hPa. The respective vertical cross section of EMAC carbon monoxide (CO) mixing ratios (Fig. 7) shows strong gradients from the boundary layer upwards and plume structures due to the biomass burning activities in boreal winter. The chosen trajectory is purely tropospheric, the 3-D model tropopause being at higher altitudes below 150 hPa, and crosses a plume layer on its way.

The dynamic situation is assessable by reducing the backward travel time of the trajectories as described in the model description for TRAJECT (Sect. 4.1). Reducing the travel time of the back trajectories reduces the number of representative trajectories necessary to describe all distinct transport pathways in a certain time interval if the thresholds for grouping the trajectories to bundles remain constant. The threshold values used here are adopted from the typical grid resolution of the 3-D model EMAC, i.e. 2.8 degrees in longitude and latitude, and a ratio of 1.1 between pressure values. As the travel time is successively reduced from five days to one day in one-day steps, the number of representative trajectories is reduced by 38, 15, 9, and 40 percent, respectively (not shown). This corresponds to the visual impression of Fig. 6: after a

<sup>5</sup>[http://www.ecmwf.int/research/era/ERA-40\\_Atlas/](http://www.ecmwf.int/research/era/ERA-40_Atlas/)

## Quantifying atmospheric transport, chemistry, and mixing

H. Riede et al.

[Title Page](#)

[Abstract](#)

[Introduction](#)

[Conclusions](#)

[References](#)

[Tables](#)

[Figures](#)



[Back](#)

[Close](#)

[Full Screen / Esc](#)

[Printer-friendly Version](#)

[Interactive Discussion](#)



frayed-out start, the trajectories converge to form the anticyclonic movement, in which less convergence and divergence take place. This is the first important reduction of representative trajectories. For the last day of fast coherent travel towards the Persian Gulf, there is a second important reduction. Monitoring the reduction of representative trajectories in different areas with changing travel times may be used as an estimate of the relative dynamics in these areas and their development with time.

## 5.2 Quantification

As we examine the full five-day trajectory, chemical species are initialised with mixing ratios interpolated from EMAC at the starting point of the trajectory five days prior to the point of observation. The time series of CO mixing ratios along the trajectory path sampled from EMAC, the CO initialisation level for CAABA/MJT, and the chemical evolution of CO within CAABA/MJT are depicted in Fig. 8. In this example, the comparatively low effective mixing ratio of CO in EMAC at the end of the trajectory is deconvolved into a small and steady negative contribution of chemistry and a strong dilutive mixing effect following the initially strong positive contribution of mixing.

Applying Eqs. (1–3) to the mixing ratios of CO and several other chemical species yields the net contributions over the whole period of five days, which are presented in Fig. 9. This condensation of information is necessary in order to evaluate comprehensive sets of trajectories, which in turn is mandatory for a statistical evaluation. However, as shown in Fig. 8, the detailed information for a closer analysis of single trajectories is available at any point along the trajectory.

The Sub-Sahel region is known for excessive biomass burning events during boreal winter. This is reflected in the elevated initialisation mixing ratios for typical biomass burning tracers such as carbon monoxide. Due to the relatively long lifetime in the upper troposphere, chemistry contributions are relatively small, where ozone is the only tracer shown to be chemically produced. There is a negative contribution of mixing to all the tracers, which takes place due to local mixing ratio maxima from biomass burning emissions at the beginning of the trajectory.

## Quantifying atmospheric transport, chemistry, and mixing

H. Riede et al.

[Title Page](#)

[Abstract](#)

[Introduction](#)

[Conclusions](#)

[References](#)

[Tables](#)

[Figures](#)

[⏪](#)

[⏩](#)

[◀](#)

[▶](#)

[Back](#)

[Close](#)

[Full Screen / Esc](#)

[Printer-friendly Version](#)

[Interactive Discussion](#)



### 5.3 Further analysis of chemistry

The robustness of the chemistry quantification with respect to the transport pathway can be assessed via ensemble plots as presented in Fig. 10.

They show the chemical evolution along EMAC and along ECMWF trajectories from the same start time interval. As expected for carbon monoxide, being a longer-lived tracer with respect to the trajectory travel time of five days, the influence of transport, i.e. initialisation, is much higher than the impact of chemistry, which shows a uniform decline. For the shorter-lived nitrogen oxides ( $\text{NO}_x$ ), much more variability due to chemistry is observed. The trajectories with high initial  $\text{NO}_x$  mixing ratios in the ECMWF ensemble compared to the EMAC ensemble originate from Suriname and the north-east coast of Brazil and show a different chemical evolution crossing the Atlantic. Consequently, the chemical evolution in similar situations has to be assessed in shorter time intervals, taking the dynamic situation into account. It needs to be stressed that mixing is only defined within the model hierarchy. Therefore, a similar uncertainty analysis is not possible for mixing.

Further analysis of chemical processes as outlined in the model description for MECCA (Sect. 4.1) is depicted in Fig. 11. Chemical contributions to production and loss of formaldehyde and carbon monoxide are evaluated based on the chemical mechanism and the reaction rates. Along the selected trajectory, formaldehyde is produced from diverse intermediates of methane oxidation and is subsequently almost exclusively transformed to carbon monoxide. Carbon monoxide, in turn, is almost exclusively produced from formaldehyde and is only chemically destroyed by hydroxyl radicals.

The chemical analysis as presented here is only applicable to chemical species which do not participate in fast cycling reaction schemes. For chemical systems with catalytic cycles, more sophisticated approaches, such as presented in Lehmann (2004) are required.

## Quantifying atmospheric transport, chemistry, and mixing

H. Riede et al.

Title Page

Abstract

Introduction

Conclusions

References

Tables

Figures



Back

Close

Full Screen / Esc

Printer-friendly Version

Interactive Discussion

## 6 Discussion

Two types of consistency are addressed in this publication: intra-model consistency between the trajectory-box model CAABA/MJT and the 3-D EMAC model, and consistency between the models and reality represented by observations or assimilated data (e.g., ECMWF, NCEP).

The intra-model consistency is based on three aspects: a common chemical and photochemical mechanism, trajectory-box model boundary conditions consistent with the 3-D model, and consistent transport in both models. The modular MESSy software structure enables convenient sharing of a common chemistry mechanism between trajectory-box model and 3-D model. Consistent transport in time and space is achieved via the calculation of trajectories based on 3-D model wind fields, and the corresponding boundary conditions are sampled from the 3-D model. The intra-model consistency is decoupled from the portability of model results to observations and can always be applied to study 3-D model characteristics including the quantification of transport, mixing, and chemistry. Using adequate models, this consistency can always be achieved.

The second consistency is the basis for the transferability of the model-based analysis to observations. It is more difficult to assess and requires additional analyses. Straightforward prerequisites to be tested are the agreement of the observations with correspondingly sampled data from the 3-D model, and the comparison of trajectories based on the 3-D model wind fields with the ones based on the forecast or reanalysis model wind fields as described in Sect. 3. Quantitatively, the simplest method to compare model results to observations is a point-to-point comparison. If 3-D data from observations are available or if a comparison with 3-D data from the forecast/reanalysis model is desired, advanced methods exist for the comparison of 3-D data fields, such as object-oriented comparisons avoiding double penalties when comparing similar atmospheric patterns that are shifted in space or time (e.g., McBride and Ebert, 2000). For the basic transferability of the meteorological situation, however, we limit the anal-

## Quantifying atmospheric transport, chemistry, and mixing

H. Riede et al.

[Title Page](#)

[Abstract](#)

[Introduction](#)

[Conclusions](#)

[References](#)

[Tables](#)

[Figures](#)



[Back](#)

[Close](#)

[Full Screen / Esc](#)

[Printer-friendly Version](#)

[Interactive Discussion](#)

ysis example here to the qualitative comparison of representative trajectories.

An interesting aspect is the exact definition of the terms transport, mixing and chemistry in this context. The definition of the contribution of transport is the most straightforward (see Sect. 2) and needs no further explanation. The contribution of chemistry is also quite intuitive as it is described by a well-defined set of chemical equations, the solution of which is only influenced by the prescribed physical boundary conditions. The definition of the mixing term is more complex. It includes all the processes and movement of air masses inside EMAC with the exception of the transport along the trajectories, such as the mixing due to vertical and horizontal diffusion, parameterised convection, scavenging, and deposition. Furthermore, it generally also includes the secondary effects of mixing onto chemistry – with the exception of chemically inert tracers (e.g., SF<sub>6</sub> as mentioned in Sect. 2). As such, the term “mixing” is meant in a broad context and is not to be confounded with “diffusive mixing” alone.

The quantification method is applied individually for each chemical species due to the specific dependence on the chemical and physical environment of each species, such as concentration gradients or sensitivity to radiation. The quantification is available at each trajectory time step of the trajectory, but can also be condensed to net contributions considering the whole trajectory.

The trajectory-box model is not confined to back trajectories and initialisation from the 3-D model. An initialisation using observational data, for instance, is possible. For the quantification method presented here, however, the consistency with the 3-D model at the start of a trajectory simulation is essential for the quantification of mixing. The choice for forward or backward trajectories is nevertheless open depending on the intended application of the quantification method.

A general improvement of input data with respect to the quality of boundary conditions for the trajectory simulations and, more importantly, of mixing ratios sampled from the 3-D model can be achieved via online sampling during the 3-D model simulation (Jöckel et al., 2009). Interpolation errors leading to artefacts in the mixing contribution are thus minimised.

## Quantifying atmospheric transport, chemistry, and mixing

H. Riede et al.

[Title Page](#)

[Abstract](#)

[Introduction](#)

[Conclusions](#)

[References](#)

[Tables](#)

[Figures](#)



[Back](#)

[Close](#)

[Full Screen / Esc](#)

[Printer-friendly Version](#)

[Interactive Discussion](#)

## 7 Summary

The model hierarchy method presented in this paper represents a new tool for the quantification of transport, chemistry, and mixing along atmospheric trajectories. A new trajectory-box model CAABA/MJT was developed, its specialty being the high consistency with respect to the 3-D global ECHAM/MESSy atmospheric-chemistry (EMAC) model. Based on the hierarchy, the separation and quantification of transport, mixing, and chemistry along atmospheric trajectories is achieved through comparisons of results from the two models. The trajectories to be analysed have to be based on the 3-D model to ensure the consistency of transport between both models. In order to achieve a sound statistical basis for results, the trajectories are grouped into coherent bundles, of which only one is used for the trajectory-box model simulations, keeping its statistical weight for future analysis.

Since data from the 3-D model is used offline, the method presented here is a time-efficient tool for on-top analysis of chemistry, mixing, and transport pathways in grid-based 3-D model simulations. The main focus, however, lies on the transfer of quantification results to observations. The transferability of quantification results to observational data is based on the comparison between representative trajectories based on the 3-D model and based on a forecast or reanalysis model, and their statistical weights. Further analysis of the spatial and temporal development of atmospheric dynamics is feasible by a variation of the backward travel time of trajectories.

The quantification method yields absolute contributions of transport, chemistry, and mixing to the mixing ratio of a species along the respective trajectory. Further analysis include an uncertainty estimate for the contributions from transport and chemistry as well as a thorough analysis of chemical processes.

*Acknowledgements.* We would like to thank H. Wernli (University of Mainz), who supplied the LAGRANTO back trajectories based on ECMWF reanalysis data and based on EMAC S1 data. H. Riede acknowledges gratefully the financial support rendered by the Max Planck Society and the International Max Planck Research School for Atmospheric Chemistry and Physics. The authors also wish to acknowledge use of the Ferret program for analysis and

## Quantifying atmospheric transport, chemistry, and mixing

H. Riede et al.

[Title Page](#)

[Abstract](#)

[Introduction](#)

[Conclusions](#)

[References](#)

[Tables](#)

[Figures](#)



[Back](#)

[Close](#)

[Full Screen / Esc](#)

[Printer-friendly Version](#)

[Interactive Discussion](#)



some graphics in this paper. Ferret is a product of NOAA's Pacific Marine Environmental Laboratory (<http://ferret.pmel.noaa.gov/Ferret/>).

The service charges for this open access publication  
5 have been covered by the Max Planck Society.

## References

Arteta, J. and Cautenet, S.: Study of ozone distribution over the south-eastern France (ES-COMPTÉ campaign): discrimination between ozone tendencies due to chemistry and to transport, *J. Atmos. Chem.*, 58, 111–130, 2007. 457

10 Jöckel, P., Sander, R., Kerkweg, A., Tost, H., and Lelieveld, J.: Technical Note: The Modular Earth Submodel System (MESSy) – a new approach towards Earth System Modeling, *Atmos. Chem. Phys.*, 5, 433–444, 2005, <http://www.atmos-chem-phys.net/5/433/2005/>. 457, 460

15 Jöckel, P., Tost, H., Pozzer, A., Brühl, C., Buchholz, J., Ganzeveld, L., Hoor, P., Kerkweg, A., Lawrence, M. G., Sander, R., Steil, B., Stiller, G., Tanarhte, M., Taraborrelli, D., van Aardenne, J., and Lelieveld, J.: The atmospheric chemistry general circulation model ECHAM5/MESSy1: consistent simulation of ozone from the surface to the mesosphere, *Atmos. Chem. Phys.*, 6, 5067–5104, 2006, <http://www.atmos-chem-phys.net/6/5067/2006/>. 457, 463

20 Jöckel, P., Kerkweg, A., Pozzer, A., Sander, R., and Tost, H.: Development cycle 2 of the Modular Earth Submodel System, *Geosci. Model Dev. Discuss.*, in preparation, 2009. 468

Kerkweg, A., Sander, R., Tost, H., Jöckel, P., and Lelieveld, J.: Technical Note: Simulation of detailed aerosol chemistry on the global scale using MECCA-AERO, *Atmos. Chem. Phys.*, 7, 2973–2985, 2007, <http://www.atmos-chem-phys.net/7/2973/2007/>. 461

25 Knudsen, B. M., Pommereau, J.-P., Garnier, A., Nunez-Pinharanda, M., Denis, L., Letrenne, G., Durand, M., and Rosen, J. M.: Comparison of stratospheric air parcel trajectories based on different meteorological analyses, *J. Geophys. Res.*, 106, 3415–3424, 2001. 460

Landgraf, J. and Crutzen, P. J.: An efficient method for online calculations of photolysis and heating rates, *J. Atmos. Sci.*, 55, 863–878, doi:10.1175/1520-0469(1998)055, 1998. 461

**GMDD**

2, 455–484, 2009

---

## Quantifying atmospheric transport, chemistry, and mixing

H. Riede et al.

---

Title Page

Abstract

Introduction

Conclusions

References

Tables

Figures

⏪

⏩

◀

▶

Back

Close

Full Screen / Esc

Printer-friendly Version

Interactive Discussion

- Lehmann, R.: An algorithm for the determination of all significant pathways in chemical reaction systems, *J. Atmos. Chem.*, 47, 45–78, 2004. 466
- McBride, J. L. and Ebert, E. E.: Verification of quantitative precipitation forecasts from operational numerical weather prediction models over Australia, *Weather Forecast.*, 15, 103–121, doi:10.1175/1520-0434(2000)015, 2000. 467
- 5 McKenna, D. S., Konopka, P., Groöb, J.-U., Günther, G., Müller, R., Spang, R., Offermann, D., and Orsolini, Y.: A new Chemical Lagrangian Model of the Stratosphere (CLaMS) 1. Formulation of advection and mixing, *J. Geophys. Res.*, 107(D16), 4309, doi:10.1029/2000JD000114, 2002. 457
- 10 Roeckner, E., Brokopf, R., Esch, M., Giorgetta, M., Hagemann, S., Kornblueh, L., Manzini, E., Schlese, U., and Schulzweida, U.: Sensitivity of simulated climate to horizontal and vertical resolution in the ECHAM5 atmosphere model, *J. Climate*, 19, 3771–3791, doi: 10.1175/JCLI3824.1, 2006. 463
- Sander, R., Kerkweg, A., Jöckel, P., and Lelieveld, J.: Technical note: The new comprehensive atmospheric chemistry module MECCA, *Atmos. Chem. Phys.*, 5, 445–450, 2005, <http://www.atmos-chem-phys.net/5/445/2005/>. 457, 461
- 15 Sander, R., Gromov, S., Harder, H., Jöckel, P., Kerkweg, A., Kubistin, D., Riede, H., Taraborrelli, D., and Xie, Z.-Q.: The atmospheric chemistry box model CAABA/MECCA-3.0, *Geosci. Model Dev. Discuss.*, in preparation, 2009. 457
- 20 Sandu, A. and Sander, R.: Technical note: Simulating chemical systems in Fortran90 and Matlab with the Kinetic PreProcessor KPP-2.1, *Atmos. Chem. Phys.*, 6, 187–195, 2006, <http://www.atmos-chem-phys.net/6/187/2006/>. 461
- Scheele, M. P., Siegmund, P. C., and Velthoven, P. F. J.: Sensitivity of trajectories to data resolution and its dependence on the starting point: in or outside a tropopause fold, *Meteorol. Appl.*, 3, 267–273, 1996. 457
- 25 Sinnhuber, B.-M., Müller, R., Langer, J., Bovensmann, H., Eyring, V., Klein, U., Trentmann, J., Burrows, J. P., and Künzi, K. F.: Interpretation of mid-stratospheric Arctic ozone measurements using a photochemical box-model, *J. Atmos. Chem.*, 34, 281–290, 1999. 457
- Stohl, A.: Computation, accuracy and applications of trajectories – a review and bibliography, *Atmos. Environ.*, 32, 947–966, 1998. 460
- 30 Stohl, A., Wotawa, G., Seibert, P., and Kromp-Kolb, H.: Interpolation errors in wind fields as a function of spatial and temporal resolution and their impact on different types of kinematic trajectories, *J. Appl. Meteorol.*, 34, 2149–2165, doi:10.1175/1520-0450(1995)034, 1995. 457

**GMDD**

2, 455–484, 2009

---

**Quantifying  
atmospheric  
transport, chemistry,  
and mixing**

H. Riede et al.

---

[Title Page](#)

[Abstract](#)

[Introduction](#)

[Conclusions](#)

[References](#)

[Tables](#)

[Figures](#)

[⏪](#)

[⏩](#)

[◀](#)

[▶](#)

[Back](#)

[Close](#)

[Full Screen / Esc](#)

[Printer-friendly Version](#)

[Interactive Discussion](#)

Stohl, A., Haimberger, L., Scheele, M. P., and Wernli, H.: An intercomparison of results from three trajectory models, *Meteorol. Appl.*, 8, 127–135, 2001. 460

Stohl, A., Forster, C., Frank, A., Seibert, P., and Wotawa, G.: Technical note: The Lagrangian particle dispersion model FLEXPART version 6.2, *Atmos. Chem. Phys.*, 5, 2461–2474, 2005, <http://www.atmos-chem-phys.net/5/2461/2005/>. 457

Wernli, H. and Davies, H. C.: A Lagrangian-based analysis of extratropical cyclones. I: The method and some applications, *Q. J. Roy. Meteor. Soc.*, 123, 467–489, doi:10.1256/smsqj.53810, 1997. 457, 463

## GMDD

2, 455–484, 2009

### Quantifying atmospheric transport, chemistry, and mixing

H. Riede et al.

Title Page

Abstract

Introduction

Conclusions

References

Tables

Figures

⏪

⏩

◀

▶

Back

Close

Full Screen / Esc

Printer-friendly Version

Interactive Discussion

## Quantifying atmospheric transport, chemistry, and mixing

H. Riede et al.

**Table 1.** Chemical production and loss reactions for formaldehyde and carbon monoxide. Turnover is given as absolute mixing ratio and as percentage of all production or of all loss for a species, respectively.

		reaction ID	turnover (pmol/mol)	turnover (%)	reaction
HCHO	production	G4104	1040.0	79.49	$\text{CH}_3\text{O}_2 + \text{NO} \rightarrow \text{HCHO} + \text{NO}_2 + \text{HO}_2$
		G4102	133.0	10.10	$\text{CH}_3\text{OH} + \text{OH} \rightarrow \text{HCHO} + \text{HO}_2$
		J4100	66.2	5.04	$\text{CH}_3\text{OOH} + h\nu \rightarrow \text{HCHO} + \text{OH} + \text{HO}_2$
		G4107	49.7	3.78	$\text{CH}_3\text{OOH} + \text{OH} \rightarrow .7 \text{CH}_3\text{O}_2 + .3 \text{HCHO} + .3 \text{OH} + \text{H}_2\text{O}$
HCHO	loss	J4101a	698.00	53.00	$\text{HCHO} + h\nu \rightarrow \text{H}_2 + \text{CO}$
		J4101b	436.00	33.14	$\text{HCHO} + h\nu \rightarrow \text{H} + \text{CO} + \text{HO}_2$
		G4108	182.00	13.84	$\text{HCHO} + \text{OH} \rightarrow \text{CO} + \text{H}_2\text{O} + \text{HO}_2$
CO	production	J4101a	698.0	52.36	$\text{HCHO} + h\nu \rightarrow \text{H}_2 + \text{CO}$
		J4101b	436.0	32.73	$\text{HCHO} + h\nu \rightarrow \text{H} + \text{CO} + \text{HO}_2$
		G4108	182.0	13.67	$\text{HCHO} + \text{OH} \rightarrow \text{CO} + \text{H}_2\text{O} + \text{HO}_2$
CO	loss	G4110	6230.00	100.00	$\text{CO} + \text{OH} \rightarrow \text{H} + \text{CO}_2$

[Title Page](#)
[Abstract](#)
[Introduction](#)
[Conclusions](#)
[References](#)
[Tables](#)
[Figures](#)
[Back](#)
[Close](#)
[Full Screen / Esc](#)
[Printer-friendly Version](#)
[Interactive Discussion](#)

## Quantifying atmospheric transport, chemistry, and mixing

H. Riede et al.

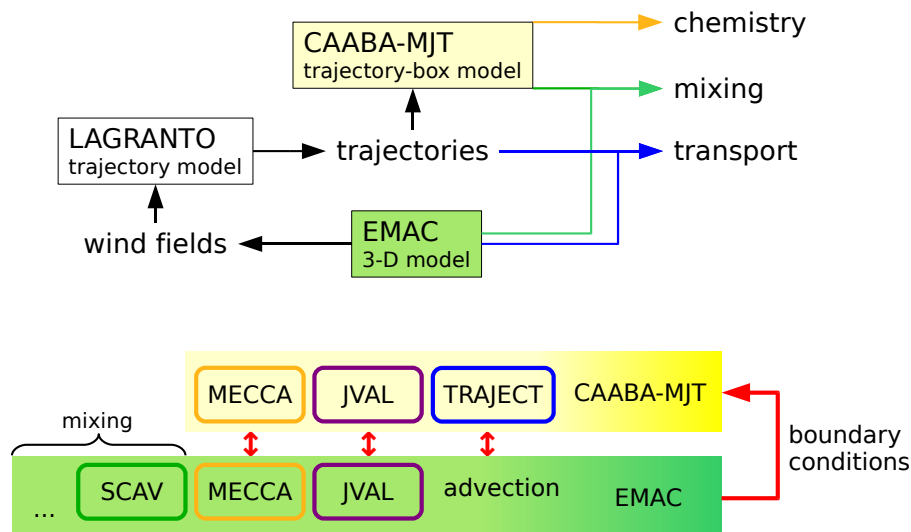


**Fig. 1.** Depiction of the model hierarchy consisting of the trajectory-box model CAABA/MJT and the global 3-D atmospheric chemistry EMAC model. Flow and combinations of model data used for the quantification of transport, chemistry, and mixing (upper part) and consistency between models (lower part, red double arrows).

Title Page

Abstract

Introduction

Conclusions

References

Tables

Figures

◀

▶

◀

▶

Back

Close

Full Screen / Esc

Printer-friendly Version

Interactive Discussion

Quantifying  
atmospheric  
transport, chemistry,  
and mixing

H. Riede et al.

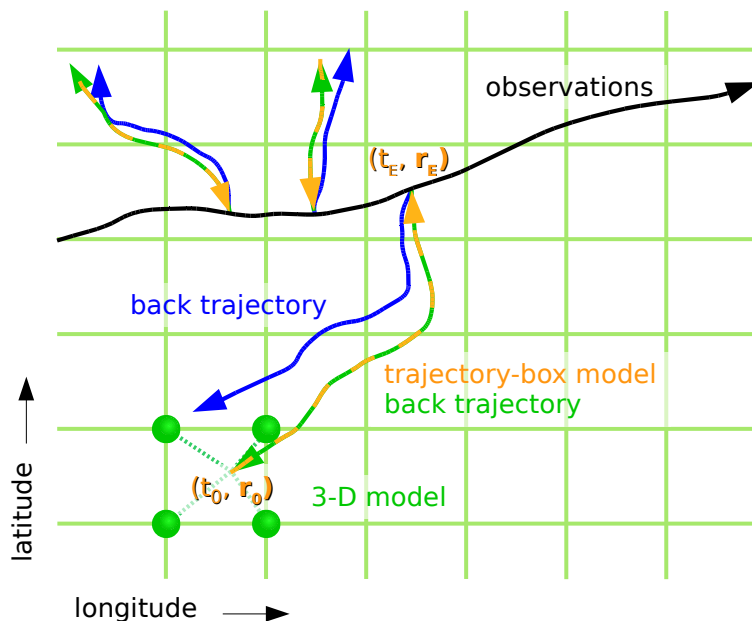


**Fig. 2.** Different models, observations, and their spatial regimes are shown. Observations are collected, in this case on a moving platform (black). Back trajectories are calculated as is often routine in campaign support (blue). In our approach, back trajectories are based on wind fields from the 3-D model (green) and chemistry is calculated forward in time (from  $t_0$  to  $t_E$ ) along the trajectories with a trajectory-box model (orange). Mixing ratios at the start of a trajectory ( $t_0$ ,  $r_0$ ) are taken from the 3-D model (green grid). The initial values are determined by interpolation (dotted green lines) between adjacent values (green dots) on the 3-D-model grid.

[Title Page](#)[Abstract](#)[Introduction](#)[Conclusions](#)[References](#)[Tables](#)[Figures](#)[◀](#)[▶](#)[◀](#)[▶](#)[Back](#)[Close](#)[Full Screen / Esc](#)[Printer-friendly Version](#)[Interactive Discussion](#)

## Quantifying atmospheric transport, chemistry, and mixing

H. Riede et al.

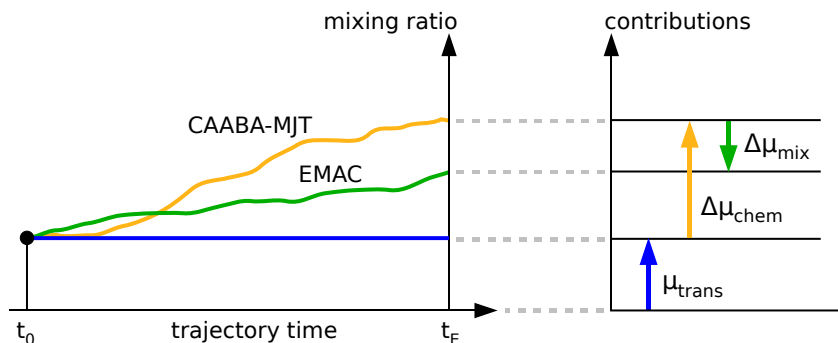


**Fig. 3.** Separation and quantification of contributions for a single trajectory is depicted schematically. The time evolution of a mixing ratio for a certain species in the two models (left) and the subsequent translation into the separate contributions of transport, mixing, and chemistry (right) are shown. In the particular example depicted here, chemical production along the trajectory is much larger than the initial value that would have been measured with transport alone, but is partly compensated by mixing.

[Title Page](#)[Abstract](#)[Introduction](#)[Conclusions](#)[References](#)[Tables](#)[Figures](#)[◀](#)[▶](#)[◀](#)[▶](#)[Back](#)[Close](#)[Full Screen / Esc](#)[Printer-friendly Version](#)[Interactive Discussion](#)

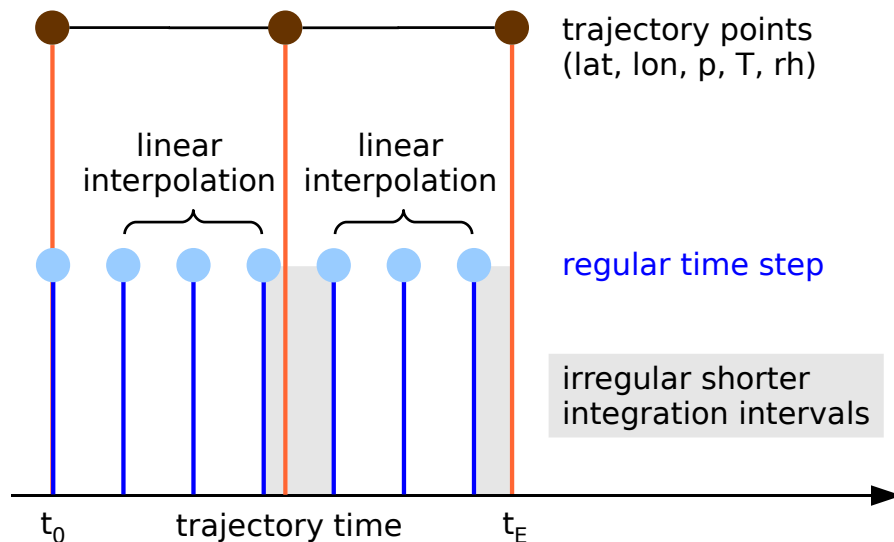


**Fig. 4.** Time stepping scheme for a single trajectory showing the trajectory points, prescribing latitude, longitude, pressure, temperature, and humidity (top, red), and the regular time steps, typically 15 min intervals (middle, blue). Regular integration points that do not coincide with a trajectory point are evaluated using linear interpolation between the trajectory points. Trajectory waypoints are always evaluated independent of the regular time stepping so that smaller time steps are inserted around trajectory points that do not coincide with a regular integration point (bottom, grey shade).

[Title Page](#)
[Abstract](#)
[Introduction](#)
[Conclusions](#)
[References](#)
[Tables](#)
[Figures](#)
[⏪](#)
[⏩](#)
[◀](#)
[▶](#)
[Back](#)
[Close](#)
[Full Screen / Esc](#)
[Printer-friendly Version](#)
[Interactive Discussion](#)

## Quantifying atmospheric transport, chemistry, and mixing

H. Riede et al.

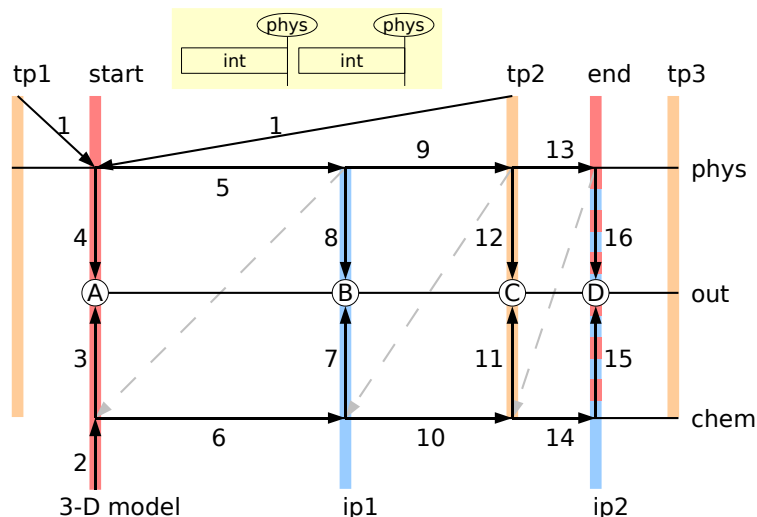


**Fig. 5.** Operator splitting scheme for the calculation of an inner section of a three-point trajectory. Physical boundary conditions are shown in the upper (phys), chemistry progress in the lower (chem), and output intervals in the middle string (out). As a first step, the starting point boundary conditions are linearly interpolated between the first (tp1) and the second (tp2) trajectory point (1). Then, chemistry is accordingly initialised with mixing ratios from the 3-D model (2). These values are written to output (3, 4, A). The boundary conditions are updated (5) before integration of the chemistry equations takes place (6) and results are output (7, 8, B). Sequence 5–8 is repeated (9–12, 13–16) on trajectory waypoints (tp2) and regular integration points (ip1, ip2) as shown in Fig. 4 until the defined end of the calculation is reached. In the shaded box, the very simplified scheme shows that each integration step is performed with the boundary conditions from the end point of the corresponding time interval.

Title Page

Abstract

Introduction

Conclusions

References

Tables

Figures

◀

▶

◀

▶

Back

Close

Full Screen / Esc

Printer-friendly Version

Interactive Discussion

---

**Quantifying  
atmospheric  
transport, chemistry,  
and mixing**

H. Riede et al.

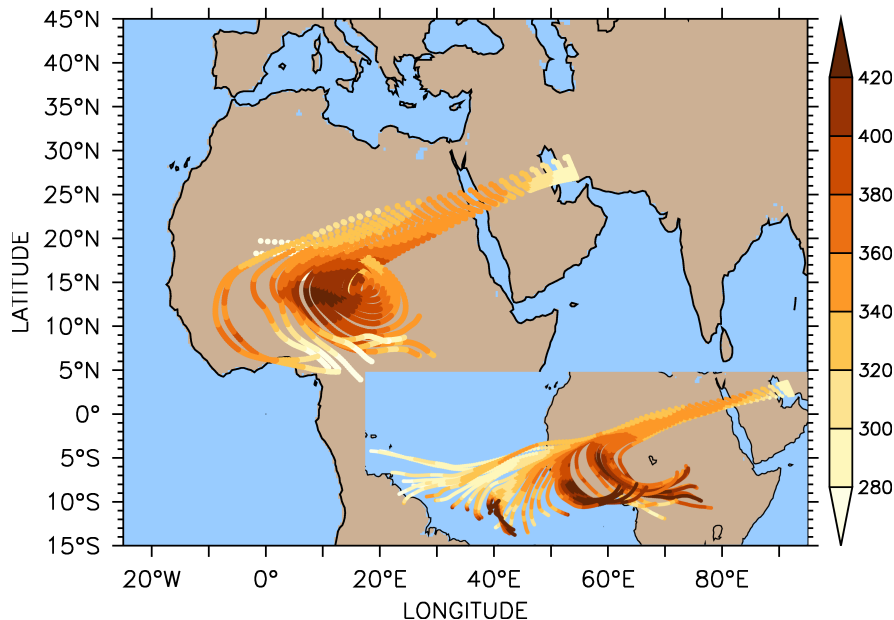


**Fig. 6.** Five-day back trajectories from the sub-Saharan region in January 2000 based on EMAC wind fields. Pressure altitude in hPa is indicated by colour. The inset shows the same five-day back trajectories based on ECMWF wind fields. Note that each each of the trajectories shown represents a bundle of 3–35 (EMAC) or 1–92 (ECMWF) coherent trajectories.

[Title Page](#)[Abstract](#)[Introduction](#)[Conclusions](#)[References](#)[Tables](#)[Figures](#)[⏪](#)[⏩](#)[◀](#)[▶](#)[Back](#)[Close](#)[Full Screen / Esc](#)[Printer-friendly Version](#)[Interactive Discussion](#)

---

**Quantifying  
atmospheric  
transport, chemistry,  
and mixing**

H. Riede et al.

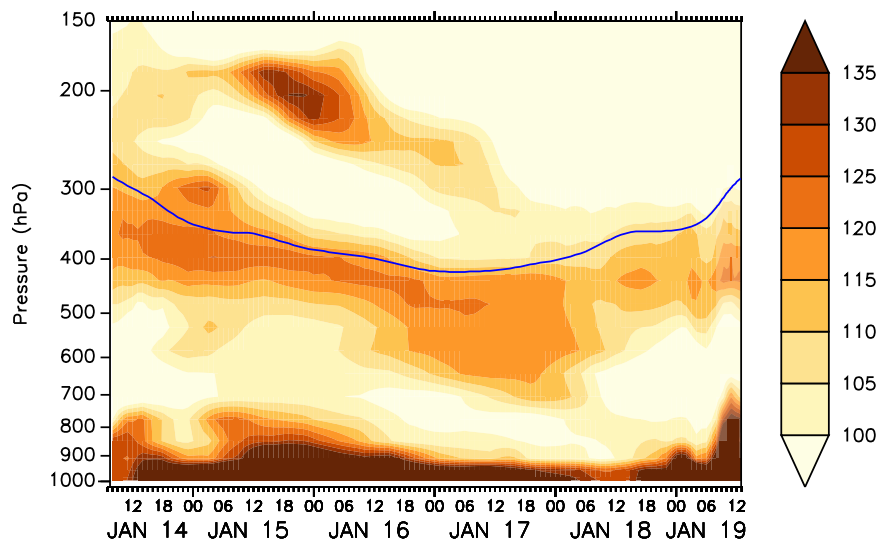


**Fig. 7.** Vertical cross section of CO mixing ratios from EMAC along the trajectory path (blue). Biomass burning activity in the sub-Sahel zone during boreal winter causes high CO gradients near the surface and CO plumes at higher altitudes.

[Title Page](#)[Abstract](#)[Introduction](#)[Conclusions](#)[References](#)[Tables](#)[Figures](#)[⏪](#)[⏩](#)[◀](#)[▶](#)[Back](#)[Close](#)[Full Screen / Esc](#)[Printer-friendly Version](#)[Interactive Discussion](#)

---

**Quantifying  
atmospheric  
transport, chemistry,  
and mixing**

H. Riede et al.

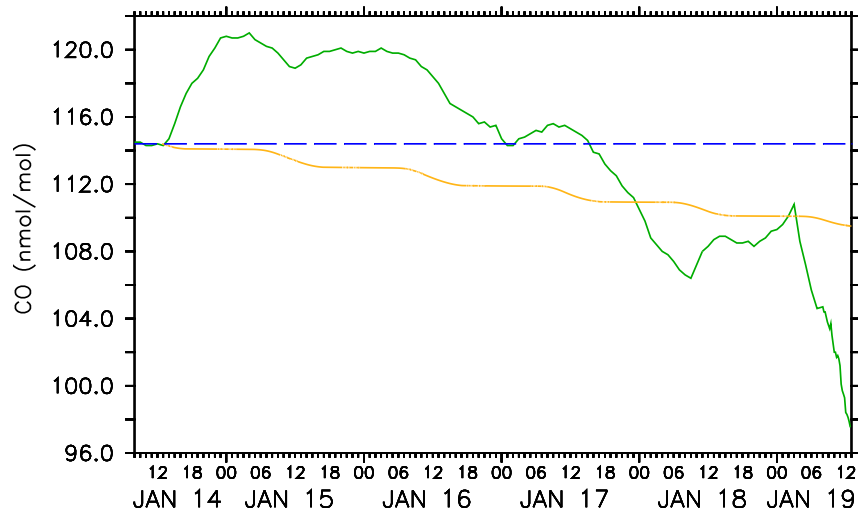


**Fig. 8.** Application example for the left part of Fig. 3. From the time series of CO mixing ratios sampled from EMAC (green solid line), the initial mixing ratio for the trajectory-box model is chosen five days prior to observations (blue dashed line). The subsequent chemical evolution calculated by CAABA/MJT is shown as orange dash-dotted line.

[Title Page](#)[Abstract](#)[Introduction](#)[Conclusions](#)[References](#)[Tables](#)[Figures](#)[⏪](#)[⏩](#)[◀](#)[▶](#)[Back](#)[Close](#)[Full Screen / Esc](#)[Printer-friendly Version](#)[Interactive Discussion](#)

## Quantifying atmospheric transport, chemistry, and mixing

H. Riede et al.

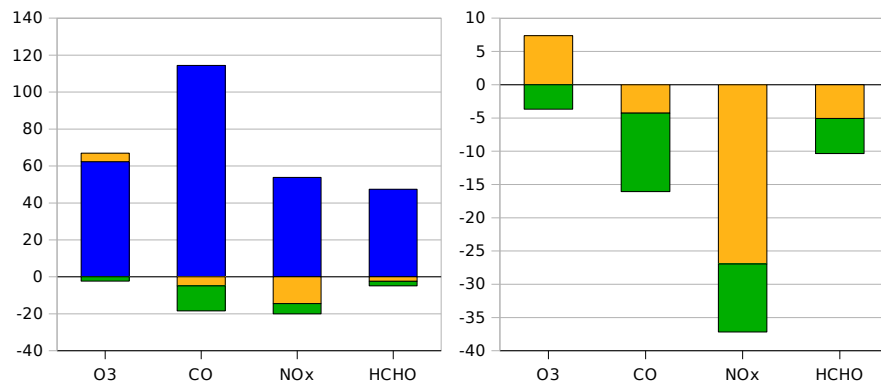


**Fig. 9.** Quantification of theoretical undisturbed transport (blue), chemistry (orange), and mixing (green), as outlined in the right part of Fig. 3, is obtained from the data presented in Fig. 8. Ozone (O<sub>3</sub>) and carbon monoxide (CO) mixing ratios are given in nmol/mol (ppbv), formaldehyde (HCHO) and the sum of nitric oxide and nitrogen dioxide mixing ratios (NO+NO<sub>2</sub>=NO<sub>x</sub>) in pmol/mol (pptv). Absolute contributions (left) and contributions in percent relative to the initial mixing ratios, i.e. undisturbed transport (right) are shown.

Title Page

Abstract

Introduction

Conclusions

References

Tables

Figures

⏪

⏩

◀

▶

Back

Close

Full Screen / Esc

Printer-friendly Version

Interactive Discussion

---

**Quantifying  
atmospheric  
transport, chemistry,  
and mixing**

H. Riede et al.

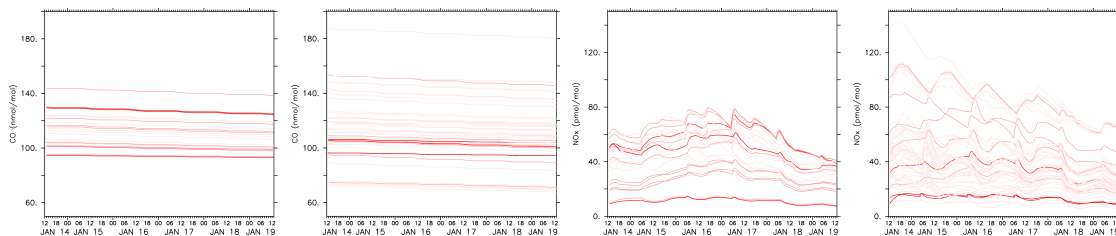


**Fig. 10.** Ensemble plot for carbon monoxide (left) and nitrogen oxides (right) simulated on trajectories based on EMAC (relative left) and ECMWF (relative right) in the same time interval. The more intense the red hue the more statistical weight the respective trajectory has.

[Title Page](#)[Abstract](#)[Introduction](#)[Conclusions](#)[References](#)[Tables](#)[Figures](#)[⏪](#)[⏩](#)[◀](#)[▶](#)[Back](#)[Close](#)[Full Screen / Esc](#)[Printer-friendly Version](#)[Interactive Discussion](#)

---

**Quantifying  
atmospheric  
transport, chemistry,  
and mixing**H. Riede et al.

---

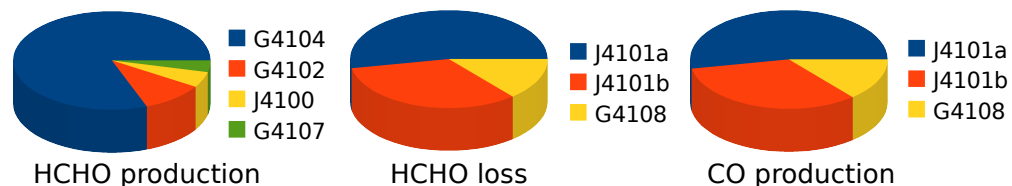


**Fig. 11.** Most important contributions of single reactions to the production of formaldehyde (left), loss of formaldehyde (middle), and production of carbon monoxide (right). The corresponding values and chemical equations are listed in Table 1.

[Title Page](#)[Abstract](#)[Introduction](#)[Conclusions](#)[References](#)[Tables](#)[Figures](#)[⏪](#)[⏩](#)[◀](#)[▶](#)[Back](#)[Close](#)[Full Screen / Esc](#)[Printer-friendly Version](#)[Interactive Discussion](#)